AD-A094 344 INDIANA UNIV AT BLOOMINGTON DEPT OF CHEMISTRY F/G 7/4
AN APPROXIMATE MODEL FOR THE LIBERATION AND IONIZATION OF ATOMS--ETC(U)
JAN 81 B D BLEASDELL, E P WITTIG, G M HIEFTJE N00014-76-C-0838
UNCLASSIFIED TR-31 NL

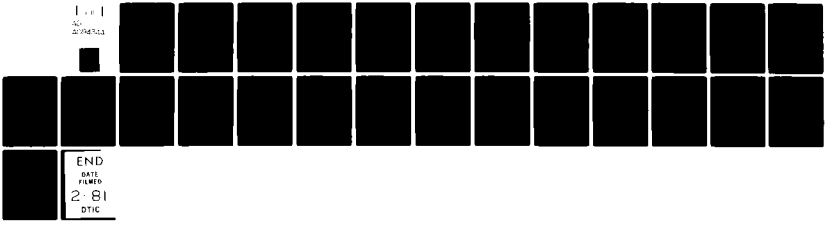

END
DATE FILMED
2-81
DTIC

UNCLASSIFIED

SECURITY CLASSIFICATION OF THIS PAGE (When Data Entered)

REPORT DOCUMENTATION PAGE

READ INSTRUCTIONS BEFORE COMPLETING FORM

1. REPORT NUMBER: THIRTY-ONE	2. GOVT ACCESSION NO.: AD-A094344
3. RECIPIENT'S CATALOG NUMBER:	
4. TITLE (and Subtitle): An Approximate Model for the Liberation and Ionization of Atoms from Individual Solute Particles in Flame Spectrometry	5. TYPE OF REPORT & PERIOD COVERED: Interim Technical Report
	6. PERFORMING ORG. REPORT NUMBER: 39
7. AUTHOR(s): B. D. Bleasdell, E. P. Wittig, and G. M. Hieftje	8. CONTRACT OR GRANT NUMBER(s): N-14-76-C-0838 / N00014-76-C-0838
9. PERFORMING ORGANIZATION NAME AND ADDRESS: Department of Chemistry, Indiana University, Bloomington, Indiana 47405	10. PROGRAM ELEMENT, PROJECT, TASK AREA & WORK UNIT NUMBERS: NR 51-622
11. CONTROLLING OFFICE NAME AND ADDRESS: Office of Naval Research, Washington, D.C.	12. REPORT DATE: 6 January 1981
	13. NUMBER OF PAGES: 21
14. MONITORING AGENCY NAME & ADDRESS (if different from Controlling Office): TR-31, 39	15. SECURITY CLASS. (of this report): UNCLASSIFIED
	15a. DECLASSIFICATION/DOWNGRADING SCHEDULE

16. DISTRIBUTION STATEMENT (of this Report)

Approved for public release; distribution unlimited

17. DISTRIBUTION STATEMENT (of the abstract entered in Block 20, if different from Report)

18. SUPPLEMENTARY NOTES

Prepared for publication in SPECTROCHIMICA ACTA, PART B

19. KEY WORDS (Continue on reverse side if necessary and identify by block number)

atom formation
flame spectrometry
atomic absorption
ionization mechanism

20. ABSTRACT (Continue on reverse side if necessary and identify by block number)

A model is described which incorporates the generation and ionization of atoms during the vaporization of individual solute particles in flames. Particles initially larger than a critical radius have two vaporization rate constants because of a change in the vaporization mechanism related to size. Consequently, the mathematical formulation of the model consists of a series of three equations which are used to curve-fit different portions of emission intensity-time profiles in an air-acetylene flame. Values for the vaporization rate constants for three alkali chlorides found for this fitting process are:

DD FORM 1 JAN 73 1473 EDITION OF 1 NOV 65 IS OBSOLETE S/N 0102-014-6601

UNCLASSIFIED

SECURITY CLASSIFICATION OF THIS PAGE (When Data Entered)

AD A094344

DTIC ELECTE FEB 2 1981 A

FILE COPY

81 2 02 153

20. (continued)

Na (244 $\mu m^2/s$, 127 $\mu m/s$), K (650 $\mu m^2/s$, 299 $\mu m/s$), and Cs (385 $\mu m^2/s$, 847 $\mu m/s$). First-order ionization rates are 58 s^{-1} for Na, 268 s^{-1} for K, and 1128 s^{-1} for Cs.

OFFICE OF NAVAL RESEARCH

Contract N14-76-C-0838

Task No. NR 051-622

TECHNICAL REPORT NO. 31

AN APPROXIMATE MODEL FOR THE LIBERATION AND IONIZATION OF ATOMS FROM INDIVIDUAL SOLUTE PARTICLES IN FLAME SPECTROMETRY

by

B. D. Bleasdell, E. P. Wittig, and G. M. Hieftje

Prepared for Publication

in

SPECTROCHIMICA ACTA, PART B

Indiana University

Department of Chemistry

Bloomington, Indiana 47405

January 26, 1981

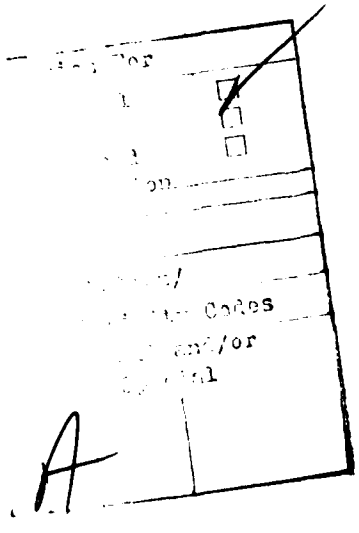

ABSTRACT

A model is described which incorporates the generation and ionization of atoms during the vaporization of individual solute particles in flames. Particles initially larger than a critical radius have two vaporization rate constants because of a change in the vaporization mechanism related to size. Consequently, the mathematical formulation of the model consists of a series of three equations which are used to curve-fit different portions of emission intensity-time profiles in an air-acetylene flame. Values for the vaporization rate constants for three alkali chlorides found for this fitting process are: Na (244 $\mu m^2/s$, 127 $\mu m/s$), K (650 $\mu m^2/s$, 299 $\mu m/s$), and Cs (385 $\mu m^2/s$, 847 $\mu m/s$). First-order ionization rates are 58 s^{-1} for Na, 268 s^{-1} for K, and 1128 s^{-1} for Cs.

In flame spectrometry, a wet aerosol of sample solution must undergo desolvation and vaporization to form the free atoms needed for analysis. During desolvation, the solvent associated with the sample evaporates, leaving behind the dry solute particle. The desolvation process has been studied previously [1]. Vaporization begins immediately after desolvation of the particle is complete; apparently both atomic and molecular species are volatilized from the surface of the dry particle. Vaporization in flames has been reported [2] to occur through either a heat or mass-transfer controlled process, depending on the composition of the solute particle. In this communication a model is proposed which closely fits experimental data on atom formation gathered in our laboratory using the isolated droplet sample introduction method [3]. Simplified calculations based on this model provide approximate but useful values for several rate constants important in the particle vaporization and atom ionization processes.

THEORY

The conclusion reached in previous studies of vaporization [2] was that there are two equations which describe the time-dependent radius of a solute particle vaporizing in an analytical flame. When the particle diameter is much larger than the mean free path of the free atoms [4] (large particle model), the equation for the radius, r, of the dry particle as a function of time, t, is similar to that for desolvation [1,2]:

$$r = (r_0^2 - k_{V1}t)^{1/2} \qquad t \leq r_0^2/k_{V1} \tag{1}$$

where r_o is the initial particle radius and k_{v1} is the vaporization rate constant for the large particle model. For particles much smaller than the mean free path of the released atoms [4] (small particle model), the equation becomes:

$$r = r_0 - k_{v2}t \qquad t < r_0/k_{v2} \tag{2}$$

where k_{v2} is the vaporization rate constant for the small particle model. Both equations are expected to be valid at particular periods during the life of a single solute particle except when the initial diameter of the particle is much smaller than the mean free path of the liberated atom. In the present case, the mean free path is of the order of 0.3-1.5 μm, as discussed later. In this latter case, only the small particle model would be valid.

The number of atoms, F, which are vaporized will be proportional to the mass vaporized (m) which, in turn, is proportional to the cube of the particle radius [2]:

$$F = \frac{Nm}{Z} = \frac{4\pi\rho N\epsilon}{3M}(r_o^3 - r^3) \tag{3}$$

where N is Avogadro's number, M is the atomic weight of the analyte, ε is the fraction of mass entering the vapor phase as free atoms (atomization efficiency), and ρ is the density of the analyte atoms in the condensed phase. Combining equations (1) and (3) for the large particle model yields

$$F = \frac{4\pi\rho N\epsilon}{3M}\left[r_o^3 - (r_o^2 - k_{v1}t)^{3/2}\right] \qquad 0 \le t \le r_o^2/k_{v1} \tag{4}$$

and for the small particle model equations (2) and (3) give

$$F = \frac{4\pi\rho N\epsilon}{3M}\left[r_o^3 - (r_o - k_{v2}t)^3\right] \qquad 0 \le t \le r_o/k_{v2} \tag{5}$$

In the vaporization of many solutes, particularly those of the alkali metals, atom loss through ionization must also be considered. For these elements, a situation exists in which there is the formation of the atomic species through vaporization of the particle and the simultaneous loss of the species by ionization. Previous studies of alkali metals [5,6] have found the ionization rate to be first order with respect to the metal. Of course, an observed loss of alkali atoms through ionization would not follow strictly first-order kinetics because of the simultaneous occurrence of ion-electron recombination, an event which opposes the ionization process. However, at short times (i.e., within two ionization time constants, $2k_i^{-1}$) after the completion of alkali particle vaporization, the contribution of ion-electron recombination to the ionization process appears to be small and constant, being caused principally by intrinsic flame electrons. During this period, the overall vaporization-ionization process for the large particle model can be represented by the following differential equation:

$$\frac{dF}{dt} = \frac{4\pi\rho N\epsilon}{3M}\left[\frac{3}{2}k_{V_1}(r_0^2 - k_{V_1}t)^{1/2}\right] - k_i F \qquad (6)$$

where F is the number of atomic species at any time (t) and k_i is the ionization rate. To solve this equation, it can be rewritten in the following form:

$$Fe^{k_i t} = \frac{4\pi\rho N\epsilon}{3M}\int \frac{3}{2}k_{V_1}(r_0^2 - k_{V_1}t)^{1/2}\, e^{k_i t}dt + C \qquad (7)$$

If the exponential term in the integral is expanded in a series and only the first term is retained, the approximate solution of equation (7) is:

$$F = \frac{4\pi\rho N\epsilon}{3M}\left[r_0^3 - (r_0^2 - k_{V_1}t)^{3/2}\right]e^{-k_i t} \tag{8}$$

The number of free atoms (F) can be related to the radiant intensity (I) they emit by

$$I = F(\alpha h\nu A)(4\pi)^{-1} \quad (W\ sr^{-1}) \tag{9}$$

where α is the fraction of atoms which are excited (Boltzmann ratio), and $h\nu$ the energy and A the emission rate (Einstein coefficient) for the observed transition. Therefore, eq. 8 can be expressed as

$$I = K\left[r_0^3 - (r_0^2 - k_{V_1}t)^{3/2}\right]e^{-k_i t} \qquad 0 \le t \le r_0^2/k_{V_1} \tag{10a}$$

and

$$I = Kr_0^3\, e^{-k_i t} \qquad t > r_0^2/k_{V_1} \tag{10b}$$

where K combines the pre-parenthetical constants in eq. 8 and the free-atom-to-intensity conversion of eq. 9.

$$K = \frac{4\pi\rho N\epsilon}{3M}\left(\frac{\alpha h\nu A}{4\pi}\right) = \frac{\rho N\epsilon\alpha h\nu A}{3M} \tag{11}$$

In actual measurements, the radiant intensity (I) is seldom measured; instead, relative emission intensity values are recorded. Consequently, the experimental value for K which is obtained includes a number of scaling factors (including measurement solid angle, optical transmission, detection efficiency, electronic gain, etc.) and can best be derived empirically. The empirical value will be designated K' in the later treatment.

A similar mathematical treatment of the small particle model is pos-

$$\frac{dF}{dt} = \frac{4\pi\rho N\varepsilon}{3M}[3k_{V_2}(r_0 - k_{V2}t)^2] - k_i F \tag{12}$$

$$Fe^{k_i t} = \frac{4\pi\rho N\varepsilon}{3M}\int 3k_{V2}(r_0 - k_{V_2}t)^2\, e^{k_i t}\, dt + C \tag{13}$$

$$F = \frac{4\pi\rho N\varepsilon}{3M}[r_0^3 - (r_0 - k_{V_2}t)^3]e^{-k_i t} \tag{14}$$

$$I = K[r_0^3 - (r_0 - k_{V_2}t)^3]e^{-k_i t} \qquad 0 \le t \le r_0/k_{V2} \tag{15}$$

and

$$I = Kr_0^3 e^{-k_i t} \qquad t > r_0/k_{V2} \tag{16}$$

In the most general case, the vaporization and ionization processes can be combined for both large and small particles in a series of equations which relate intensity to the initial particle radius and to a parameter we have termed the critical radius, r_c. The critical radius is that hypothetical particle size at which control of vaporization in the model appears to change from the large particle to the small particle mechanism. The relationship of the critical radius to the critical time, t_c, and the time of complete vaporization, t_f, can be found from equations (17) and (18).

$$t_c = (r_0^2 - r_c^2)/k_{v_1} \qquad r_0 \geq r_c \tag{17}$$

$$t_f = (r_0^2 - r_c^2)/k_{v_1} + r_c/k_{v_2} \qquad r_0 \geq r_c \tag{18}$$

The three equations required to describe the entire vaporization-ionization process for the combined model are:

$$I = K[r_0^3 - (r_0^2 - k_{v_1}t)^{3/2}]e^{-k_i t} \qquad 0 \leq t \leq t_c \tag{19}$$

$$I = K[r_0^3 - (r_c - k_{v_2}[t - t_c])^3]e^{-k_i t} \qquad t_c < t \leq t_f \tag{20}$$

$$I = Kr_0^3 e^{-k_i t} \qquad t > t_f \tag{21}$$

Equation (19) is valid for the time period ($0 \leq t \leq t_c$) when the vaporization process follows the large particle model (equation (10A)). During the time period when the vaporization process follows the small particle model (equation (20)) , the total number of free atoms (neglecting ionization) is the sum of those from the large-particle vaporization process which occurred earlier, i.e., $K[r_0^3 - r_c^3]$, and those from the continuing small particle vaporization described by equation (15). Note that it is necessary to redefine the time scale used in that portion of equation (20) which deals with the small particle vaporization because the small particle

vaporization model is not employed until after the completion of the large particle model, i.e., $t > t_c$. Therefore, the time becomes $t - t_c$ in equation (20) when the free atoms are being formed; however, in the ionization term, $e^{-k_i t}$, time is still defined from the beginning of the initial particle vaporization because ionization decreases the total free atom population at all times. After the completion of vaporization, $t > t_f$, equation (21) will be valid as long as the ionization process is first-order and the ion-electron recombination process is negligible!

EXPERIMENTAL

To study the vaporization process, emission intensity-time profiles were obtained using the droplet generator system originally described by Hieftje and Malmstadt [3]. In this technique, droplets are individually and reproducibly injected into an air-acetylene flame in such a manner that one views an individual droplet and its products without interference or influence from products of neighboring droplets.

The air-acetylene flame was supported on a modified Meker burner [1] and was operated at an air flow of 15.0 L/min and an acetylene flow of 2.25 L/min. The velocity of the flame was determined to be 11 m/s [7]. A quartz sheath, 17.5 cm above the burner top, was used to stabilize the flame [8]. The plume of emitting vapor products was focused without magnification onto the entrance slit (200 μm) of a 0.35 m monochromator (Model EU 700, Heath Co., Benton Harbor, MI), which was tipped on end so the entrance slit intercepted a complete horizontal cross-section of the flame image. The emission signal was detected by a R928 photomultiplier tube (Hammamatsu Corp.,

Middlesex, NJ) operated at -800 V and the resulting current measured by a picoammeter (414S, Keithley Instruments, Inc., Cleveland, OH). Data from the picoammeter were collected by a PDP 12/40 computer (Digital Equipment Corp., Maynard, MA). To eliminate the effects of flame temperature variations, the optical system was fixed in position to monitor the emission signal at a constant height in the flame (19 cm above the burner top). To obtain the temporal behavior of the emission intensity, the droplet generator was scanned vertically under computer control by means of a stepper motor (SM-2A, Denco Research, Inc., Tucson, AZ) and a lead screw connected to the droplet generator mount.

Solutions of the chlorides were prepared from dried reagent grade chemicals according to standard procedures [9].

Droplet diameters were measured by the MgO impression technique [10]. The initial dried particle radius, r_o, was calculated indirectly from the initial droplet diameter, solution concentration (64 μg/mL in all cases), and the crystalline solute density (NaCl, 2.165 g/mL; KCl, 1.984 g/mL; CsCl, 3.988 g/mL).

RESULTS AND DISCUSSION

Figure 1 shows the experimental emission intensity-time curve obtained for a 64 μg/mL potassium solution. To qualitatively describe this curve it is convenient to divide it into three regions as shown in the figure:
Region A) At the beginning of the vaporization process, the emission intensity increases rapidly (vaporization rate is proportional to Ar^2) as free atoms and other species are volatilized from the surface of the particle.

Ionization is also occurring in this region and will serve to decrease the emitting atom population. Region B) In the second region, the vaporization process continues (the vaporization rate is now proportional to Δr) to produce free atoms and other species while ionization continues to remove the emitting atoms. The combination of the slower production and the continual removal of the free atoms causes a slowing in the rate of growth of the emission intensity. Region C) At the completion of the vaporization process there is the continued removal of the free atoms through the ionization process. This results in a decrease in the emission intensity.

In order to fit equations 19-21 to an experimental curve, it is necessary to obtain values for K', k_{v1}, k_i, t_c, r_c, k_{v2}, and t_f. These values are calculated from five data points selected from the experimental curve (cf., for example, Fig. 1). The first data point is located at the beginning of vaporization ($t = 0$, $I = 0$). The second point is chosen on the rapidly rising portion of the curve, near the beginning of vaporization. A third point is selected near the maximum intensity. The foueth and fifth points are chosen a short time beyond the maximum intensity where vaporization is presumed to be complete. Only the choice of data point one is critical ($t = 0$, $I = 0$); the others are used only to calculate approximate values of the desired parameters and establish approximate time zones (large particle behavior, small particle behavior, time after completion of vaporization) which are necessary to define the regions for these calculations. An outline of the method is described below.

After vaporization is complete (region C). In this region, where only ionization is occurring, k_i and K' can be calculated from experimental data points 4 and 5 using equation (21):

$$k_i = [1/(t_4 - t_5)] \ln(I_5/I_4) \qquad t_5 > t_4 > t_f \tag{22}$$

$$K' = (I_4/r_0^3)e^{k_i t_4} \qquad t_4 > t_f \tag{23}$$

Large particle time period (region A). In this region, k_{v1} can be calculated from experimental data point 2 using equation (19) and the values calculated from equations (22) and (23).

$$k_{v1} = \frac{1}{t_2}\left[r_0^2 - \left(r_0^3 - \left\{\frac{I_2}{K'}\right\}e^{k_i t_2}\right)^{2/3}\right] \qquad 0 < t_2 \leq t_c \tag{24}$$

Small particle time period (region B). To calculate k_{v2}, a value for r_c is necessary. The critical radius is conveniently set initially at zero (large particle model) and iteratively increased to yield the best calculated fit to the experimental data points. A value of t_c can now be calculated from equation (17). With this value of t_c and experimental data point 3, it is possible to calculate first k_{v2} (equation (25)) and t_f (equation (18)) using equation (20):

$$k_{v2} = \frac{1}{(t_3 - t_c)}\left[r_c - \left(r_0^3 - \left\{\frac{I_3}{K'}\right\}e^{k_i t_3}\right)^{1/3}\right] \qquad t_c < t_3 \leq t_f \tag{25}$$

Two things should be noted concerning the method of calculating the unknown parameters as described above: (1) the experimental data point(s) used to calculate a specific parameter must fall within the time zone where that calculation is valid; (2) once a value has been calculated for each

of the curve-fit parameters and the time zones established, any desired number of data points (we normally use 15 for the entire curve) can be assigned to the appropriate time zones and the corresponding curve-fit parameter can be calculated and averaged for all data points that fall within that time zone.

Figure 2 demonstrates the improvement in curve-fit which the combined model provides over either the large or small particle model for droplets of a 64 μg/mL potassium solution. The various curve-fit parameters for each of the three models based on Fig. 2 are shown in Table 1. The difference in intensity between each experimental data point and the calculated value is squared and summed for all of the experimental data points. This value is reported as the Σ (residual)^2 in Table 1. The sum of the squares of the residuals for the combined model indicates dramatically improved agreement with observations over both the large and small particle models.

In Figs. 3 and 4, experimental data points and the combined-model curve are shown for vaporization of a particle derived from solutions of 64 μg/mL sodium and 64 μg/mL cesium, respectively. The combined-model parameters for these emission intensity profiles are compiled in Table 2. The accuracy of vaporization rates cited in Tables 1 and 2 is limited by the use of approximate solutions to differential equations (6) and (12). In a comparison of these results with an exact numeric solution of the differential equations, we have found an error in calculated vaporization rates up to 10%. However, the simplicity of the present treatment and its utility for calculating ionization rates renders such a possible error acceptable in many cases. Work is currently underway to evaluate numerically the vaporization rate constants for each of the alkali metals. Importantly, the error associated with the

present approximation is determinate, and will be greatest for metals which exhibit the most ionization (e.g., Cs).

Few of the parameters calculated form this model and reported in Tables 1 and 2 can be compared with literature values because, for the most part, such values do not exist. The values of the ionization rate constants reported here are in rough agreement with those reported in other flames [11]. The values of the particle diameters corresponding to the critical radii yielding the best curve fits for sodium, potassium and cesium are 0.88 μm, 0.86 μm, and 0.64 μm, respectively. Using appropriate values of the diffusion coefficients for the elements as reported by SNELLEMAN [12], values of the mean free path for sodium, potassium and cesium are calculated to be 0.77 μm, 0.55 μm, and 1.29 μm, respectively [4]. These differences between critical diameters and mean free paths could be due to some uncertainty in the values of the diffusion coefficients and/or the effect of combining the large and small particle models in such a manner that the change from one model to the other is abrupt in our treatment whereas in a real system the change would be gradual.

CONCLUSION

In this study a combined vaporization-ionization model for single solute particles in flames is described. This model provides a new method for the determination of the rates of ionization and particle vaporization. For the first time, approximate vaporization rate constants for three alkali chlorides are reported. Although the model has only been applied to a selected number of elements, it is believed to be of general utility for

systems which exhibit first-order ionization. The model can, however, cause large systematic errors in calculated vaporization rates when the ionization rates are large. Work with exact numeric solutions of the differential equations are being examined in more detail.

REFERENCES

1. N. C. Clampitt and G. M. Hieftje, Anal. Chem., 44, 1211 (1972).
2. G. J. Bastiaans and G. M. Hieftje, Anal. Chem., 46, 901 (1974).
3. G. M. Hieftje and H. V. Malmstadt, Anal. Chem., 40, 1860 (1968).
4. P. W. Jacobs and A. Russel-Jones, J. Phys. Chem., 72, 202 (1968).
5. A. F. Ashton and A. N. Hayhurst, Combust. Flame, 21, 69 (1963).
6. Tj. Hollander, P. J. Kalff and C. Th. J. Alkemade, J. Chem. Phys., 39, 2558 (1963).
7. C. B. Boss, and G. M. Hieftje, Appl. Spectrosc. 32, 377 (1978).
8. G. M. Hieftje and R. I. Bystroff, Spectrochim. Acta, Part B, 30, 187 (1975).
9. Dean and T. Rains, Flame Emission and Atomic Absorption Spectroscopy, Dean and T. Rains, Chapter 13, "Standard Solutions for Flame Spectrometry," Marcel Dekker (1969) New York.
10. K. R. May, J. Sci. Instrum., 27, 128 (1950).
11. D. E. Jensen and P. J. Padley, Trans. Faraday Soc., 62, 2140 (1966).
12. W. Snelleman, Ph.D. Thesis, University of Utrecht, 1965.

TABLE 1. Vaporization and ionization parameters for potassium. Emission profiles obtained from 27.5 μm diameter droplets containing 64 μg/mL of potassium as the chloride salt.

Parameter	Definition	Model			Ref. 11
		Large Particle	Small Particle	Combined	
k_1 (s^{-1})	ionization rate constant	247	247	268	165,150[+]
k_{v1} ($\mu m^2/s$)	large particle vaporization rate constant	579	---	650	
k_{v2} (μm/s)	small particle vaporization rate constant	---	515	299	
t_f (ms)	time of complete vaporization	0.50	1.05	1.60	
t_c (ms)	critical time	---	---	0.16	
r_o[*] (μm)	initial dried particle radius	0.54	0.54	0.54.	
r_c (μm)	critical particle radius	---	---	0.43	
Σ (residual)^2		1580	1122	78	

[*]Calculated based on solution concentration, an assumed density of 1.984 g/mL, and an initial droplet diameter of 27.5 μm.

[+]$H_2 + O_2 + N_2$ flame at 2440 K

TABLE 2. Vaporization and ionization parameters for sodium and cesium emission profiles obtained from 27.5 μm droplets containing 64 μg/mL of each element as the chloride salt.

Parameter	Sodium	Cesium	Sodium Ref. 11	Cesium Ref. 11
k_i (s^{-1})	58	1128	50[†]	270,290[†]
k_{v1} ($\mu m^2/s$)	244	385		
k_{v2} ($\mu m/s$)	127	847		
t_f (ms)	4.04	0.49		
t_c (ms)	0.59	0.11		
r_o (μm)	0.58	0.58		
r_c (μm)	0.44	0.32		
χ^2 (residual)^2	18	12		

[†] $H_2 + O_2 + N_2$ flame at 2440 K

FIGURE LEGENDS

Figure 1. Five representative data points and calculated intensity-time curve for volatilization of a particle obtained from a 27.5 μm droplet containing 64 μg/mL potassium as KCl. ⊡ are the experimental data points. The points are from the three time zones; A, large particle vaporization region; B, small particle vaporization zone; and C, time after vaporization is complete. Point 1 is taken at the beginning of vaporization, t = 0, I = 0. Point 2 is chosen before the critical time, t_c. Point 3 is chosen near the maximum. Points 4 and 5 are chosen after the time, t_v, when vaporization is complete.

Figure 2. Experimental data points and calculated intensity-time curves for vaporization of particles obtained from a solution of 64 μg/mL potassium. Initial droplet diameter is 27.5 μm. ⊡ are the experimental data points. L is the calculated curve for the large particle model. S is the calculated curve for the small particle model. C is the calculated curve for the combined model.

Figure 3. Experimental data points and the combined model curve-fit for vaporization of particles obtained from a 64 μg/mL sodium solution. The initial droplet size is 27.5 μm. ⊡ are the experimental data points.

Figure 4. Experimental data points and the combined model curve-fit for vaporization of particles obtained from a 64 μg/mL cesium solution. Initial droplet diameter is 27.5 μm. ⊡ are the experimental data points.

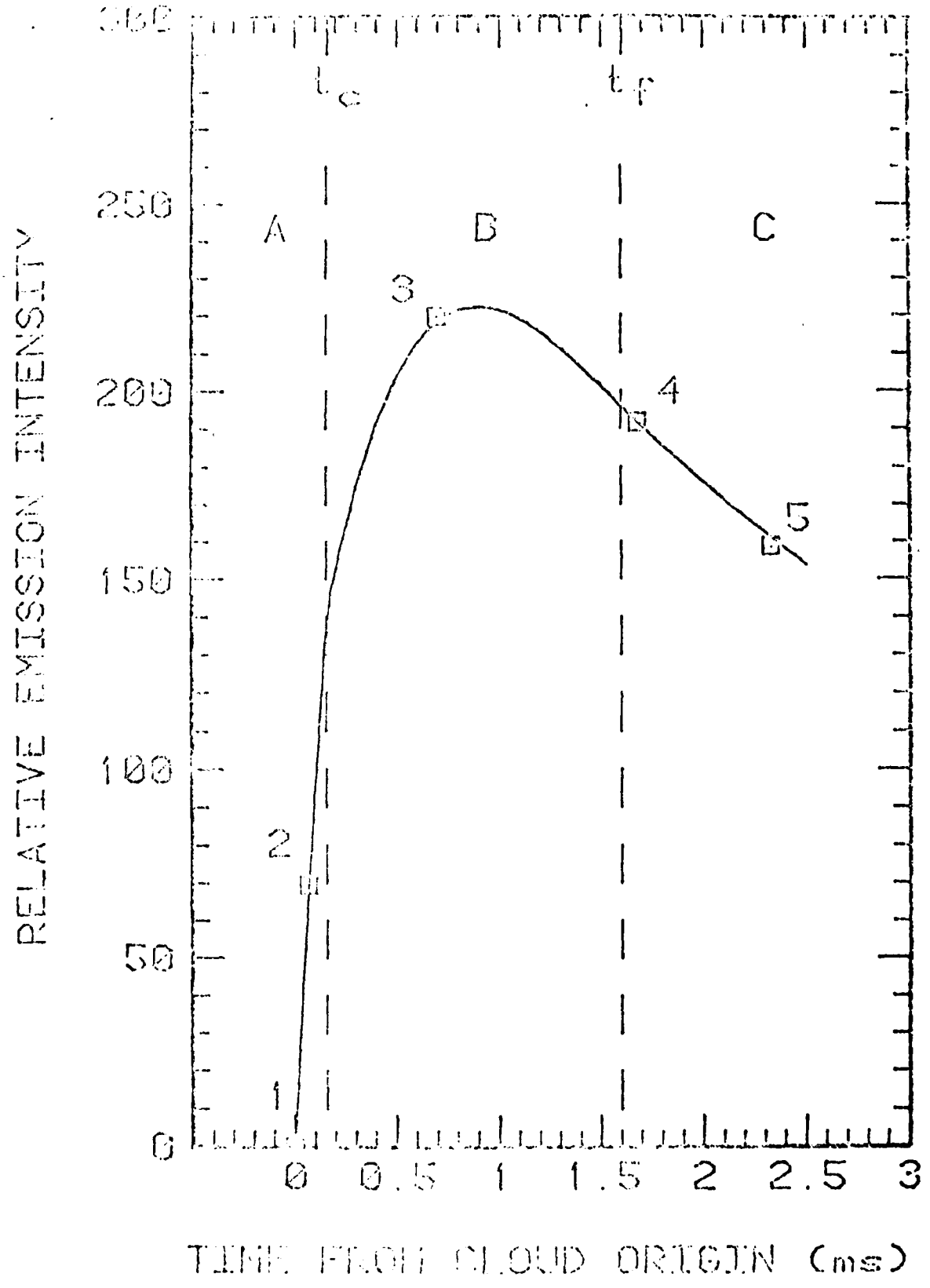
300
250
200
150
100
50
0
RELATIVE EMISSION INTENSITY
t_c
t_f
A
B
C
1
2
3
4
5
0
0.5
1
1.5
2
2.5
3
TIME FROM CLOUD ORIGIN (ms)

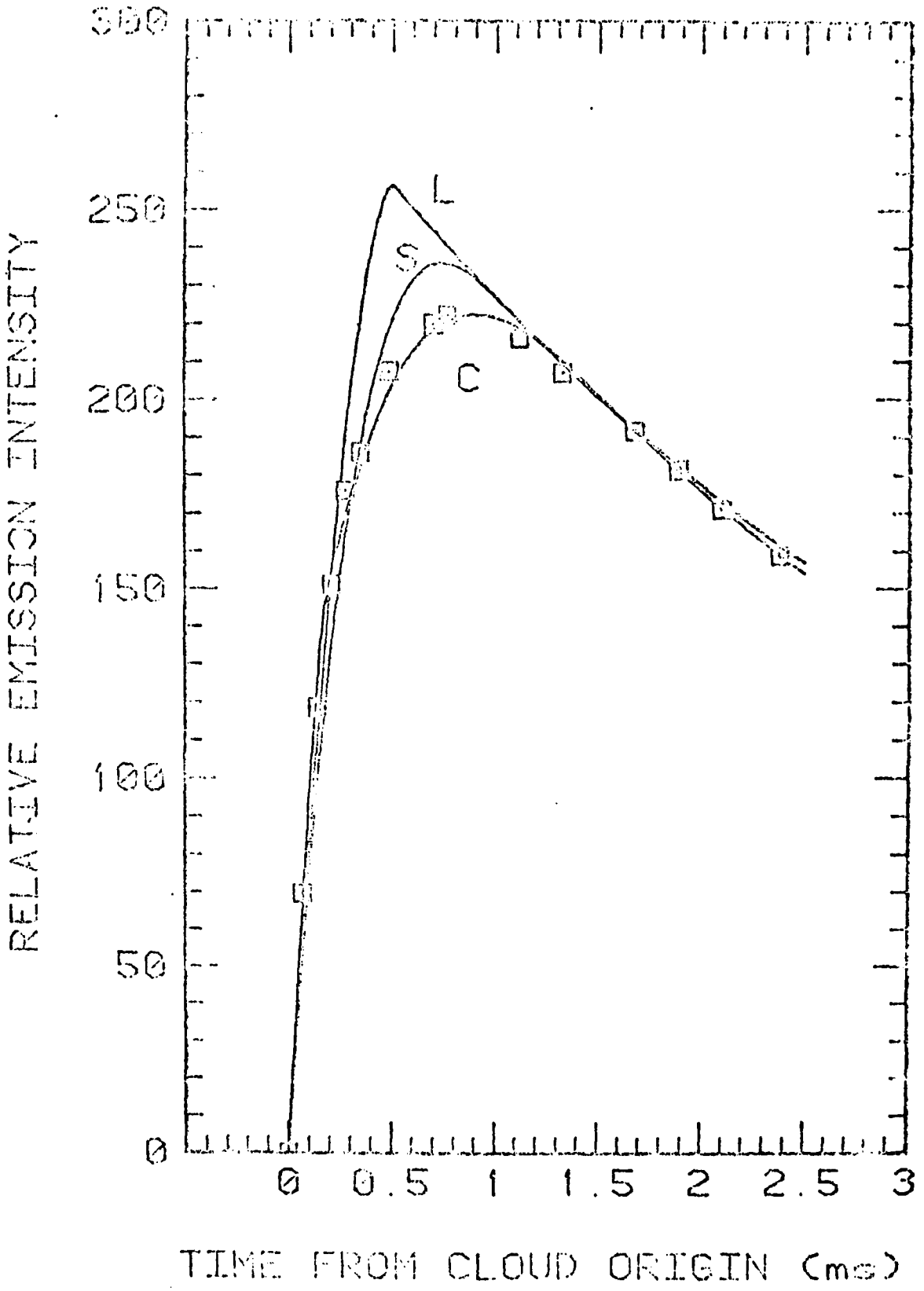
300
250
200
150
100
50
0
L
S
C
RELATIVE EMISSION INTENSITY
0
0.5
1
1.5
2
2.5
3
TIME FROM CLOUD ORIGIN (ms)

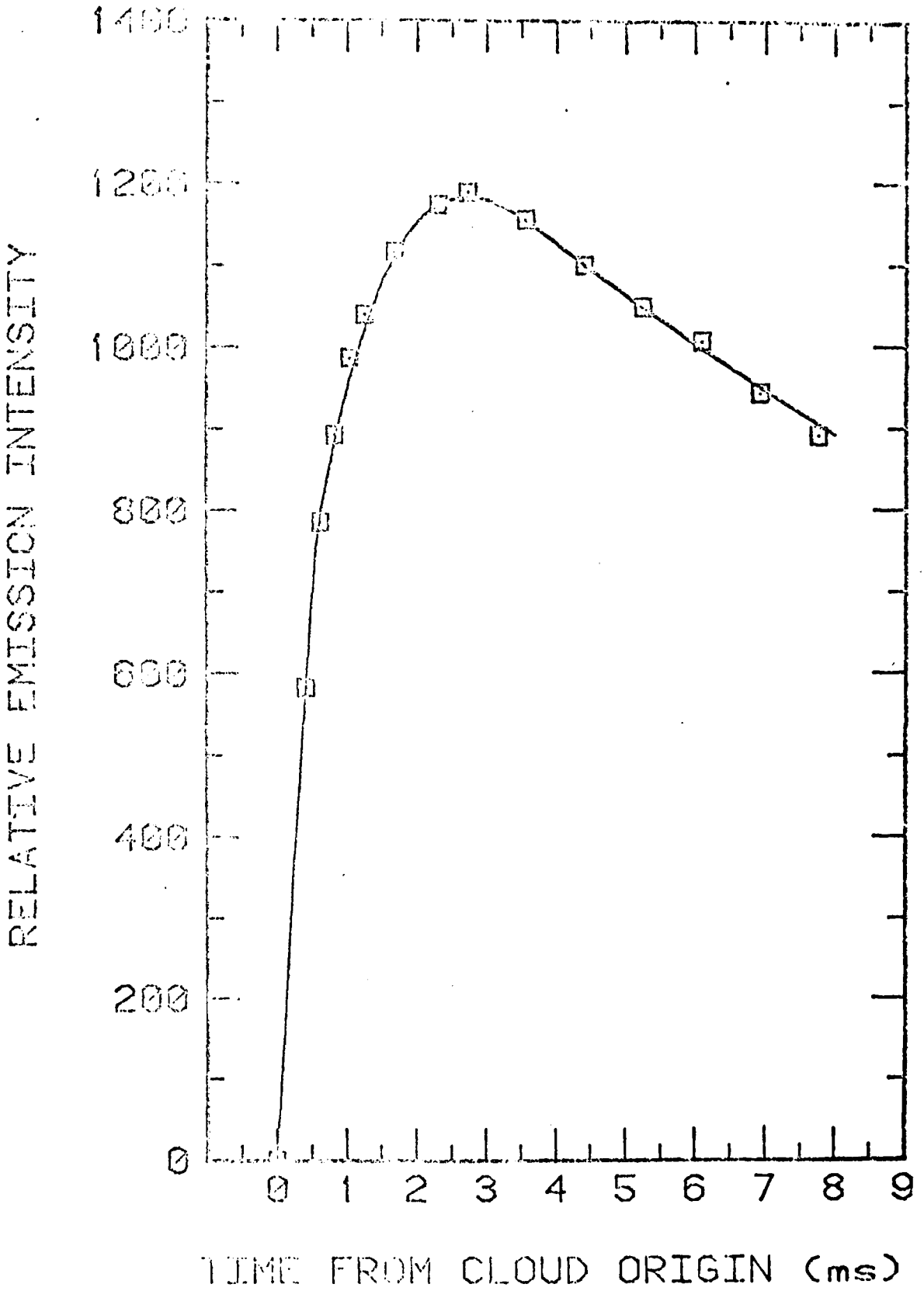
1400
1200
1000
800
600
400
200
0
RELATIVE EMISSION INTENSITY
0 1 2 3 4 5 6 7 8 9
TIME FROM CLOUD ORIGIN (ms)

SP472-3/B1

472:GAN:716:ddc
78u472-608

TECHNICAL REPORT DISTRIBUTION LIST, 051C

	No. Copies
Dr. M. B. Denton Department of Chemistry University of Arizona Tucson, Arizona 85721	1
Dr. E. A. Osteryoung Department of Chemistry State University of New York at Buffalo Buffalo, New York 14214	1
Dr. B. P. Lowalski Department of Chemistry University of Washington Seattle, Washington 98105	1
Dr. S. P. Perone Department of Chemistry Purdue University Lafayette, Indiana 47907	1
Dr. D. L. Venezky Naval Research Laboratory Code 6130 Washington, D.C. 20375	1
Dr. H. Freiser Department of Chemistry University of Arizona Tuscon, Arizona 85721	
Dr. Fred Saalfeld Naval Research Laboratory Code 6110 Washington, D.C. 20375	1
Dr. H. Chernoff Department of Mathematics Massachusetts Institute of Technology Cambridge, Massachusetts 02139	1
Dr. K. Wilson Department of Chemistry University of California, San Diego La Jolla, California	1
Dr. A. Zirino Naval Undersea Center San Diego, California 92132	1
Dr. John Duffin United States Naval Postgraduate School Monterey, California 93940	1
Dr. G. M. Hieftje Department of Chemistry Indiana University Bloomington, Indiana 47401	1
Dr. Victor L. Rehn Naval Weapons Center Code 3813 China Lake, California 93555	1
Dr. Christie G. Enke Michigan State University Department of Chemistry East Lansing, Michigan 48824	1
Dr. Kent Eisentraut, MBT Air Force Materials Laboratory Wright-Patterson AFB, Ohio 45433	1
Walter G. Cox, Code 3632 Naval Underwater Systems Center Building 148 Newport, Rhode Island 02840	1
Professor Isiah M. Warner Texas A&M University Department of Chemistry College Station, Texas 77840	1
Professor George H. Morrison Cornell University Department of Chemisty Ithaca, New York 14853	1
Dr. Rudolph J. Marcus Office of Naval Research Scientific Liaison Group American Embassy APO San Francisco 96503	1
Mr. James Kelley DTNSRDC Code 2803 Annapolis, Maryland 21402	1

TECHNICAL REPORT DISTRIBUTION LIST, GEN

	No. Copies
Office of Naval Research Attn: Code 472 800 North Quincy Street Arlington, Virginia 22217	2
ONR Branch Office Attn: Dr. George Sandoz 536 S. Clark Street Chicago, Illinois 60605	1
ONR Area Office Attn: Scientific Dept. 715 Broadway New York, New York 10003	1
ONR Western Regional Office 1030 East Green Street Pasadena, California 91106	1
ONR Eastern/Central Regional Office Attn: Dr. L. H. Peebles Building 114, Section D 666 Summer Street Boston, Massachusetts 02210	1
Director, Naval Research Laboratory Attn: Code 6100 Washington, D.C. 20390	1
The Assistant Secretary of the Navy (RE&S) Department of the Navy Room 4E736, Pentagon Washington, D.C. 20350	1
Commander, Naval Air Systems Command Attn: Code 310C (H. Rosenwasser) Department of the Navy Washington, D.C. 20360	1
Defense Technical Information Center Building 5, Cameron Station Alexandria, Virginia 22314	12
Dr. Fred Saalfeld Chemistry Division, Code 6100 Naval Research Laboratory Washington, D.C. 20375	1
U.S. Army Research Office Attn: CRD-AA-IP P.O. Box 1211 Research Triangle Park, N.C. 27709	1
Naval Ocean Systems Center Attn: Mr. Joe McCartney San Diego, California 92152	1
Naval Weapons Center Attn: Dr. A. B. Amster, Chemistry Division China Lake, California 93555	1
Naval Civil Engineering Laboratory Attn: Dr. R. W. Drisko Port Hueneme, California 93401	1
Department of Physics & Chemistry Naval Postgraduate School Monterey, California 93940	1
Dr. A. L. Slafkosky Scientific Advisor Commandant of the Marine Corps (Code RD-1) Washington, D.C. 20380	1
Office of Naval Research Attn: Dr. Richard S. Miller 800 N. Quincy Street Arlington, Virginia 22217	1
Naval Ship Research and Development Center Attn: Dr. G. Bosmajian, Applied Chemistry Division Annapolis, Maryland 21401	1
Naval Ocean Systems Center Attn: Dr. S. Yamamoto, Marine Sciences Division San Diego, California 91232	1
Mr. John Boyle Materials Branch Naval Ship Engineering Center Philadelphia, Pennsylvania 19112	1


DATE
FILMED
8